Does Ca^{2+} Reach Millimolar Concentrations after Single Photon Absorption in *Drosophila* Photoreceptor Microvilli?

Marten Postma, Johannes Oberwinkler, and Doekele G. Stavenga
Department of Neurobiophysics, University of Groningen, Nijenborgh 4, NL-9747 AG Groningen, The Netherlands

ABSTRACT The quantum bump, the elementary event of fly phototransduction induced by the absorption of a single photon, is a small, transient current due to the opening of cation-channels permeable to Ca^{2+}. These channels are located in small, tube-like protrusions of the cell membrane, the microvilli. Using a modeling approach, we calculate the changes of free Ca^{2+} concentration inside the microvilli, taking into account influx and diffusion of Ca^{2+}. Independent of permeability ratios and Ca^{2+} buffering, we find that the free Ca^{2+} concentrations rise to millimolar values, as long as we assume that all activated channels are located in a single microvillus. When we assume that as much as 25 microvilli participate in a single bump, the free Ca^{2+} concentration still reaches values higher than 80 μM. These very high concentrations show that the microvilli of fly photoreceptors are unique structures in which the Ca^{2+} signaling is even more extreme than in calcium concentration microdomains very close to Ca^{2+} channels.

INTRODUCTION

Many cell types use changes in cytosolic free calcium concentration ($[Ca^{2+}]_i$) for intracellular signaling (Berridge, 1998). Often, the changes of $[Ca^{2+}]_i$ are spatially and temporally restricted, thereby allowing a multitude of processes in one cell to be differentially regulated by $[Ca^{2+}]_i$ (Neher, 1998). Many cell types, especially neurons, have evolved dedicated mechanisms to better control and localize changes of $[Ca^{2+}]_i$. Often, cells localize Ca^{2+} channels to specialized compartments, like synaptic spines (Koch and Zador, 1993; Petrozzino et al., 1995) or the stereocilia of vertebrate hair cells (Denk et al., 1995; Lumpkin and Hudspeth, 1995). In such an arrangement, Ca^{2+} currents cause high local Ca^{2+} concentrations while a spread of Ca^{2+} into the rest of the cell body is limited.

Fly photoreceptor cells also exhibit strong localization of Ca^{2+} permeable cation channels, called transient receptor potential (TRP) and TRP-like (TRPL). In these cells, light absorption by rhodopsin triggers a PLC-mediated signaling pathway that leads—via not fully understood processes—to the opening of TRP and TRPL channels (Hardie and Minke, 1995; Montell, 1998). All known components of this signaling pathway, including the channels themselves, are situated in or very close to the microvilli (Niemeyer et al., 1996; Huber et al., 1996a; Tsunoda et al., 1997; Chevesich et al., 1997), very slender, tube-like protrusions of the photoreceptor membrane (Boschek, 1971; Hardie, 1985).

TRP and TRPL channels have been shown to be highly permeable to Ca^{2+} (Hardie and Minke, 1992; Reuss et al., 1997); therefore, light stimulation leads to localized Ca^{2+} influx into the microvilli from which Ca^{2+} diffuses into the cell body (Ranganathan et al., 1994). Prolonged stimulation with bright light leads to massive Ca^{2+} influx and to sustained concentrations in the cell body that might be higher than 20 μM (Hardie, 1996; Oberwinkler and Stavenga, 1998). This Ca^{2+} influx is functionally highly relevant because it causes an initial positive feedback at light onset followed by a subsequent negative feedback on the light response (Hardie, 1991, 1995; Hardie and Minke, 1994).

Fly photoreceptor cells exhibit an exquisite sensitivity, because the absorption of a single photon causes already a pronounced response, a so-called quantum bump (Wu and Pak, 1978; Hardie, 1991; Hardie and Minke, 1995; Hofstee et al., 1996). In this paper, we investigate the changes of ion concentrations in the microvilli during a quantum bump. Forced by the small dimensions of the microvilli, we adopt a modeling strategy to tackle this problem, including as many physiologically realistic parameters as possible. The results show that, during a quantum bump, the free calcium concentration inside the microvilli changes dramatically, possibly reaching millimolar concentrations. This emphasizes and urges the reconsideration of the importance of Ca^{2+} in shaping and regulating the photoresponse of fly photoreceptor cells, even at low light intensities.

MATERIALS AND METHODS

The model

We approximate a quantum bump, i.e., the current caused by absorption of a single photon, measured in *Drosophila* photoreceptor cells under voltage clamp (Hardie and Minke, 1995), by a Γ-function (Fig. 1),

$$I(t) = A \frac{e^p}{p^p} \left(\frac{t}{\tau}\right)^p e^{-t/\tau}, \quad (1)$$

with amplitude $A = -9.0$ pA, time constant $\tau = 4.0$ ms and parameter $p = 2.38$. It is unknown how many microvilli contribute to a quantum bump. When all the channels conducting the current are located within one microvillus, the current in that microvillus, I_m, equals the quantum bump

Received for publication 22 February 1999 and in final form 19 July 1999.
Address reprint requests to Dr. Marten Postma, Department of Neurobiophysics, University of Groningen, Nijenborgh 4, 9747 AG Groningen, The Netherlands. Tel.: +31-50-363-4771; Fax: +31-50-363-4740; E-mail: postma@bcn.rug.nl.

0006-3495/99/10/1811/13 $2.00

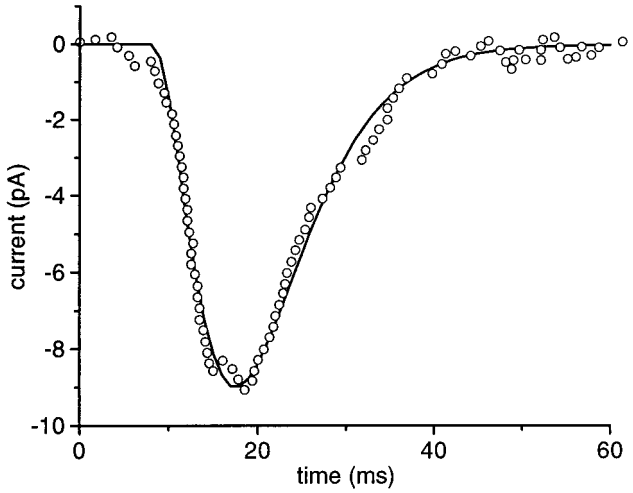

FIGURE 1 Average of 10 quantum bumps measured under voltage clamp in a *Drosophila* photoreceptor cell (*open symbols*; from Hardie and Minke, 1995), together with the fitted gamma function (Eq. 1), with parameters $A = -9$ pA, $\tau = 4.0$ ms and $p = 2.38$ (*solid line*). The fit is used as input during the simulations.

current given by Eq. 1. When n microvilli participate and the current is equally distributed over these microvilli, then $I_m(t) = I(t)/n$.

Under physiological conditions, the quantum bump in *Drosophila* is carried by four cation types, Na^+, K^+, Ca^{2+}, and Mg^{2+} (Hardie and Minke, 1992; Reuss et al., 1997),

$$I_m = I_{Na} + I_K + I_{Ca} + I_{Mg} = \sum_q I_q, \tag{2}$$

with q indicating the ion types. I_q, the current of ion type q, is the surface integral of the ion current density, i_q,

$$I_q = \int_{S_m} i_q \, dS, \tag{3}$$

where $S_m = \pi d_m L_m$ is the surface of the microvillus membrane (Fig. 2). The current density i_q is associated with the ion flux density j_q by

$$i_q = F z_q j_q, \tag{4}$$

with F the Faraday constant and z_q the valence of ion type q, i.e., $z_{Na} = z_K = 1$ and $z_{Ca} = z_{Mg} = 2$. The ions flowing through the membrane cause changes in the ion concentrations in the microvilli. These concentration changes result in concentration gradients causing ions to diffuse to (or from) the soma along the length of the microvilli. The resulting ion concentrations inside the microvillus are determined by the flux-diffusion equation,

$$\frac{\partial C_{q,i}(x)}{\partial t} = -\frac{2}{r_m} j_q(x) + D_q \nabla^2 C_{q,i}(x), \tag{5}$$

where $C_{q,i}(x)$ is the concentration of ion type q inside the microvillus at location x, $r_m = d_m/2$ is the radius of the microvillus, and D_q is the diffusion coefficient for ion type q. The factor $2/r_m$ is the surface-to-volume ratio of a cylinder with radius r_m. The microvilli are slender cylinders, closed on one side and connected by a narrow neck with the photoreceptor cell soma (Fig. 2). Considering the diffusion coefficients given in Table 1, the time τ_d necessary for a particle to diffuse an average distance x equal to the radius of the microvillus, $x = r_m$, is smaller than 3 μs ($\tau_d = \pi x^2/4D$), whereas, for an average distance equal to the microvillus length $x = L_m$, τ_d is 2–5 ms. This shows that only diffusion along the length of the microvillus needs to be taken into account considering the duration of the bump.

The ion flux density is proportional to the ion permeability P_q,

$$j_q = P_q f_q. \tag{6}$$

Assuming the validity of the Goldman–Hodgkin–Katz-current equation, f_q is given by

$$f_q(x) = \beta_q V_m \frac{C_{q,i}(x) - C_{q,o}(x) e^{-\beta_q V_m}}{1 - e^{-\beta_q V_m}} \quad \beta_q = \frac{z_q F}{RT}, \tag{7}$$

where $C_{q,o}(x)$ is the ion concentration outside the microvillus; R is the ideal gas constant and T the absolute temperature; V_m is the membrane potential. Note that an outward current is positive.

In the case of the light-activated channels of *Drosophila*, the ratios w_q of the ion permeabilities P_q and the total permeability $P_l = \Sigma P_q$, i.e., $w_q = P_q/P_l$, are known (Hardie and Minke, 1992; Reuss et al., 1997). When the permeability P_l is assumed independent of the position x, i.e., equal along the length of the microvillus, its value can be calculated from the measured current (e.g., Gerster, 1997),

$$P_l = \frac{I_m}{\varepsilon}, \tag{8}$$

where

$$\varepsilon = \pi d_m F \sum_q z_q w_q \int_0^{L_m} f_q(x) \, dx. \tag{9}$$

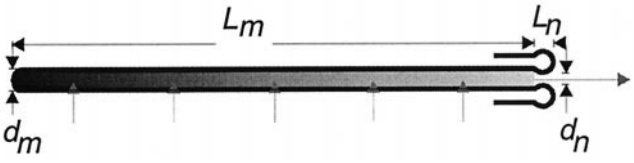

FIGURE 2 Diagram of a single *Drosophila* microvillus. A microvillus is a tube-like protrusion from the photoreceptor cell body, with average length $L_m = 1.5$ μm and diameter $d_m = 0.06$ μm, connected through a narrow neck, of length $L_n = 0.06$ μm and diameter $d_n = 0.035$ μm, to the cell soma. Upon light activation, cation channels open, giving rise to ionic fluxes through the microvillus membrane. These ionic fluxes, in combination with diffusion of ions through the neck into the cell soma, lead to concentration profiles in the microvillus.

Parameter values

The quantum bumps, yielding the average quantum bump of Fig. 1 (Hardie and Minke, 1995), were measured with the following extracellular ionic concentrations (in mM): $[Ca^{2+}]_o = 1.5$, $[Na^+]_o = 120$, $[K^+]_o = 5.0$, $[Mg^{2+}]_o = 4.0$ (Hofstee et al., 1996). Intracellular ion concentrations are not necessarily identical to the ion concentrations in the patch pipette, because the cells may transport ions into or out of the cell, and diffusion between the patch pipette and the cell may not be fast enough for the ion concentrations to equilibrate. We therefore chose $[Ca^{2+}]_i = 1.6 \cdot 10^{-4}$ mM, the value measured in dark-adapted *Drosophila* photoreceptor cells (Hardie, 1996). The Na^+/Ca^{2+}-exchanger needs to work permanently to keep $[Ca^{2+}]_i$ at this concentration; therefore, we worked with a slightly elevated $[Na^+]_i = 8.0$ mM. In the patch pipette 2.0 mM $MgSO_4$ and 4.0 mM MgATP were present; because ATP chelates Mg^{2+}, we used $[Mg^{2+}]_i = 3.0$ mM. For the intracellular potassium concentration, we used the value in the patch pipette, $[K^+]_i = 140.0$ mM (Hofstee et al., 1996). Throughout the calculations, the extracellular ion concentrations were

TABLE 1 Parameters and their values used in the calculations

Parameter	Definition	Value	Reference
T	temperature	293 K	Hofstee et al., 1996
$[Na^+]_o$	extracellular sodium concentration	120.0 mM	Hofstee et al., 1996
$[K^+]_o$	extracellular potassium concentration	5.0 mM	Hofstee et al., 1996
$[Ca^{2+}]_o$	extracellular calcium concentration	1.5 mM	Hofstee et al., 1996
$[Mg^{2+}]_o$	extracellular magnesium concentration	4.0 mM	Hofstee et al., 1996
$[Na^+]_i$	intracellular sodium concentration	8.0 mM	see text
$[K^+]_i$	intracellular potassium concentration	140.0 mM	Hofstee et al., 1996
$[Ca^{2+}]_i$	intracellular calcium concentration	$1.6 \cdot 10^{-4}$ mM	Hardie, 1996
$[Mg^{2+}]_i$	intracellular magnesium concentration	3.0 mM	see text
V_m	holding membrane potential	−70 mV	Hofstee et al., 1996
L_m	length of microvillus	1.5 μm	Hardie, 1985
d_m	diameter of microvillus	0.06 μm	Hardie, 1985
L_n	length of microvillus neck	0.06 μm	Suzuki et al., 1993
d_n	diameter of microvillus neck	0.035 μm	Boschek, 1971
D_{Na}	diffusion coefficient of sodium	650 $\mu m^2 s^{-1}$	Kushmerick and Podolsky, 1969
D_K	diffusion coefficient of potassium	1000 $\mu m^2 s^{-1}$	Kushmerick and Podolsky, 1969
D_{Ca}	diffusion coefficient of calcium	220 $\mu m^2 s^{-1}$	Albritton et al., 1992
D_{Mg}	diffusion coefficient of magnesium	200 $\mu m^2 s^{-1}$	see text
D_{cam}	diffusion coefficient of buffer	100 $\mu m^2 s^{-1}$	see text
[cam]	concentration of buffer (calmodulin)	0.5 mM	Porter et al., 1993
K_1	1. macroscopic Ca^{2+} binding constant	800 mM^{-1}	Maune et al., 1992
K_2	2. macroscopic Ca^{2+} binding constant	200 mM^{-1}	Maune et al., 1992
K_3	3. macroscopic Ca^{2+} binding constant	70 mM^{-1}	Maune et al., 1992
K_4	4. macroscopic Ca^{2+} binding constant	40 mM^{-1}	Maune et al., 1992
K_{PS}	Ca^{2+} dissociation constant of PS	83.3 mM	McLaughlin et al., 1981
$K_{PE,PC}$	Ca^{2+} dissociation constant of PE,PC	333.3 mM	McLaughlin et al., 1981

assumed to stay constant, as were the concentrations in the cell soma. These assumptions are justified by the huge difference in volume of a microvillus ($4.2 \cdot 10^{-21}$ m^3) and that of a cell body ($3.9 \cdot 10^{-15}$ m^3; Hardie, 1996) or the intraommatidial cavity.

In the calculations, we assume that the microvillus (Fig. 2) has a length $L_m = 1.5$ μm and diameter $d_m = 0.06$ μm and that the neck has a length $L_n = 0.06$ μm (Suzuki et al., 1993) and diameter $d_n = 0.035$ μm (Boschek, 1971; Hardie, 1985). For the diffusion coefficients of the ions in the microvillus we take $D_{Na} = 650$ $\mu m^2 s^{-1}$, $D_K = 1000$ $\mu m^2 s^{-1}$ (Kushmerik and Podolsky, 1969), $D_{Ca} = 220$ $\mu m^2 s^{-1}$ (Albritton et al., 1992) and $D_{Mg} = 200$ $\mu m^2 s^{-1}$ (calculated with limiting conductivity values for the Mg^{2+}- versus Ca^{2+}-ion; Robinson and Stokes, 1959). The parameter values used in the calculations are summarized in Table 1.

The holding potential of the cell yielding Fig. 1 was −70 mV. Whether the clamp also holds for the microvillar membrane depends on the length constant of the microvillus: $\lambda = \sqrt{r_m R_m/(2R_i)}$, with R_m the specific membrane resistance and R_i the specific resistance of the cytoplasm. Possible space clamp problems are most severe at the peak of the bump current. With a peak current I = −9 pA and an electromotive force $V_m - E_{rev} = -70 - 9 = -79$ mV (Reuss et al., 1997) the peak conductance is $g = 111$ pS, yielding $R_m = 25$ Ωcm^2 when assuming that the current is restricted to a single microvillus. With $R_i = 70$ Ωcm (Rall, 1977), we find that the minimal length constant of a microvillus is 7.5 μm, resulting in a voltage difference between the tip and the neck of, at most, 1.5 mV. This shows that the space clamp of the microvillar membrane is indeed present to a very good approximation.

The permeability ratios of the two light-dependent channel types of the *Drosophila* photoreceptor, TRP and TRPL, are given in Table 2, together with those for the mixture of TRP and TRPL channels encountered in the wild-type photoreceptor cells under divalent free conditions (values from Reuss et al., 1997). The permeability ratios for wild-type photoreceptor cells under physiological conditions have not been determined. However, the flash responses obtained from photoreceptor cells of the *trpl* mutant are (under physiological conditions) indistinguishable from those from wild-type flies (Niemeyer et al., 1996; Reuss et al., 1997). This argues that the permeability ratios in wild-type flies under physiological conditions are largely identical to those found for the TRP channels in the *trpl* mutants. Nevertheless, we first investigate the effects of different permeability ratios.

RESULTS

Permeability, ion currents, and concentration changes

We calculate the time course of the light-induced permeability P_l using the Γ-function (Eq. 1) fitted to the quantum bump of Fig. 1 and the parameter values given in Table 1. Figure 3 shows the results for the three different permeability ratios (Table 2) investigated. The resulting light-induced permeability is highest with all channels being TRP (case 1, Table 2), and it is almost three times lower with all channels being TRPL (case 3, Table 2). This can be explained by considering that P_l is inversely proportional to the sum of all permeability ratios w_q each multiplied by f_q (Eqs. 8 and 9). In case of the TRP channels, the large w_{Ca} dominates, but it is multiplied with a low f_{Ca} resulting in a high permeability

TABLE 2 Permeability ratios of channels for the three investigated cases*

Case	Channels	w_{Ca}	w_{Mg}	w_{Na}	w_K
1	TRP	0.88	0.10	0.01	0.01
2	TRP/TRPL	0.85	0.11	0.02	0.02
3	TRPL	0.58	0.20	0.11	0.11

*Values from Reuss et al., 1997.

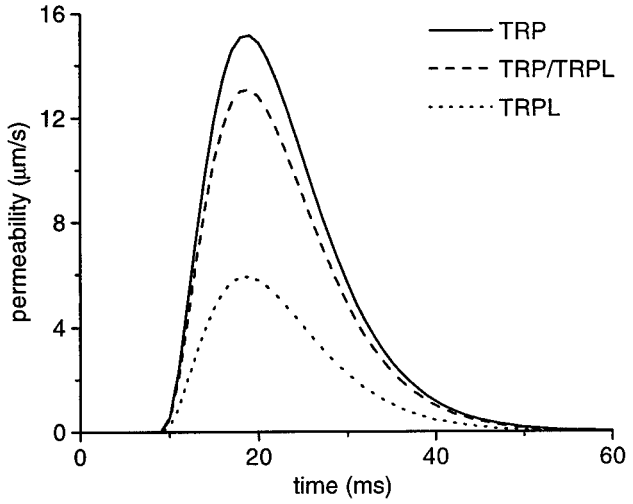

FIGURE 3 Time course of the total light-activated permeability, P_l, during a quantum bump for three different permeability ratios (Table 2).

P_l. In contrast, when we consider TRPL channel permeability ratios, w_{Na} dominates, which is multiplied by a high f_{Na} giving a smaller permeability P_l. At the membrane potential $V_m = -70$ mV, the values of the f_q are mainly determined by the extracellular ion concentrations. Hence, the difference between f_{Ca} and f_{Na} results from the lower value of $[Ca^{2+}]_o$ compared to $[Na^+]_o$.

Equally, the currents for each ion type (Fig. 4) depend on the assumed permeability ratios (Table 2). The permeability ratios of TRP channels (case 1) lead to a high proportion of the total current being carried by Ca^{2+}. The permeability ratios of TRPL channels (case 3) yield a fourfold increase in the Na^+ current compared to the TRP channel permeability ratios, whereas the Ca^{2+} current is reduced by a factor of 3. The permeability ratios of TRP and TRPL combined (case 2) always give intermediate values.

In Fig. 5, the calculated spatiotemporal profiles of the ion concentrations in the microvillus are shown, considering only TRP channels (case 1). The shapes of the spatiotemporal profiles for the other permeability ratios investigated (Table 2) are similar (data not shown). For quantitative comparison, we calculated the spatial average of the concentration profiles. The time courses of the spatially averaged ion concentrations are presented in Fig. 6. Kinetically, the concentration changes are almost perfectly paralleling the shape of the light-induced current (Figs. 1, 4, and 5). This is caused by the diffusion being rapid (2–5 ms), compared to the changes in light-induced current that last tens of milliseconds. The concentration changes for Na^+, Mg^{2+}, and also for Ca^{2+}, are in the millimolar range for the three cases studied (Table 2). The concentration of K^+ changes only very little, because the holding potential $V_m = -70$ mV is close to the Nernst potential of potassium $E_K = -84$ mV.

Previous estimates and measurements of $[Ca^{2+}]_i$ have suggested that $[Ca^{2+}]_i$ might be especially high close to the mouth of Ca^{2+} channels, in so-called microdomains (Llinás et al., 1995; Neher, 1998). However, even there $[Ca^{2+}]_i$ is

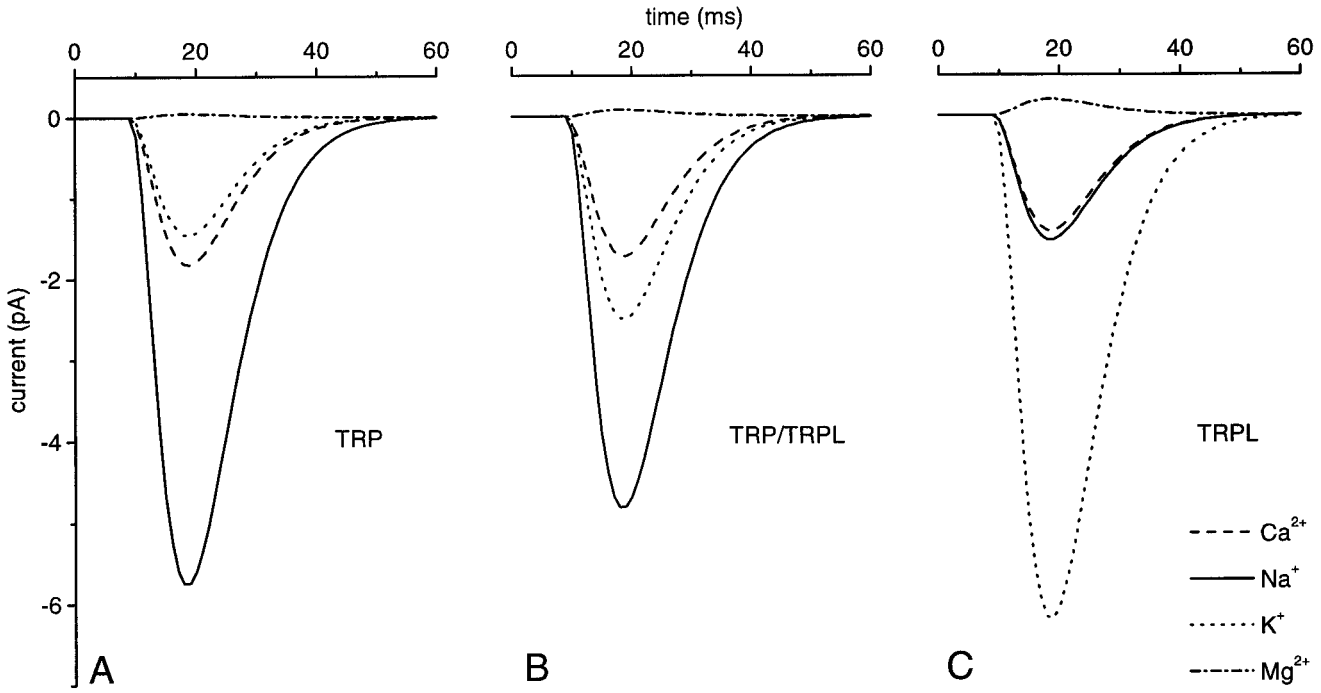

FIGURE 4 Light-induced currents of Na^+, K^+, Ca^{2+}, and Mg^{2+}, assuming permeability ratios of (*A*; case 1, Table 2) TRP channels, (*B*; case 2, Table 2) a mixture of TRP and TRPL channels, and (*C*; case 3, Table 2) TRPL channels.

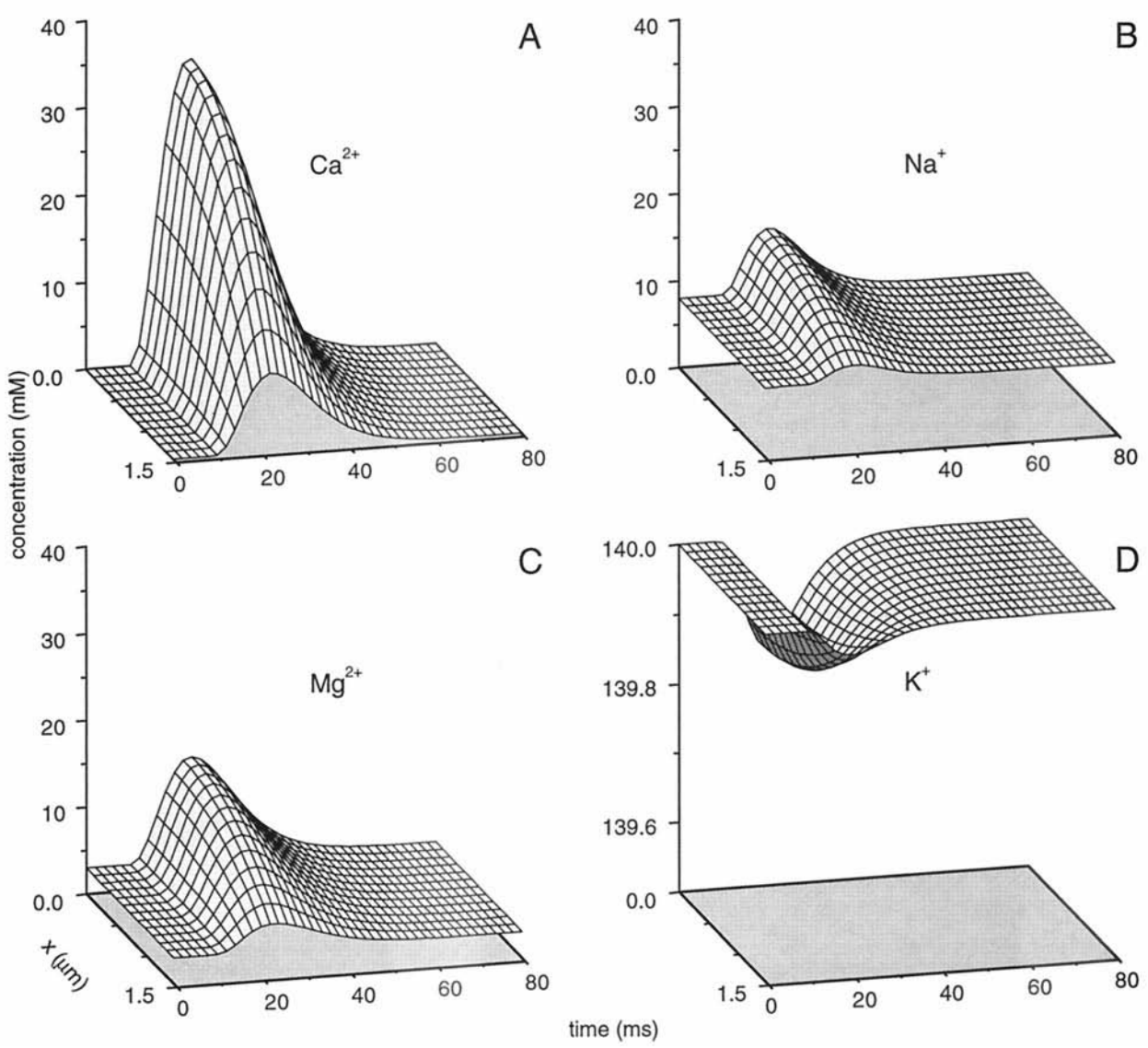

FIGURE 5 Time course of concentration profiles in a microvillus for (*A*) Na^+, (*B*) K^+, (*C*) Ca^{2+}, and (*D*) Mg^{2+}, calculated for the permeability ratios of TRP channels (case 1, Table 2); the current is assumed to flow through one single microvillus. For Na^+, Ca^{2+}, and Mg^{2+}, the bump leads to concentration changes in the millimolar range in the microvillus.

thought not to rise higher than 2.0 mM at most (Llinás et al., 1992; Roberts, 1994; Aharon et al., 1994); the $[Ca^{2+}]_i$ values calculated above seem, therefore, extraordinarily high. In the following, we thus investigate factors that might have led to an overestimation of $[Ca^{2+}]_i$ in the microvilli.

High affinity Ca^{2+} buffer

So far, we neglected the influence of calcium buffering. Fly microvilli contain 0.5 mM calmodulin (Porter et al., 1993). This high concentration and the limited space in a microvillus suggest that calmodulin might be the most important Ca^{2+} binding protein present. Calmodulin has four binding sites with different affinities. The steady-state binding can be described by an Adair–Klotz equation (Maune et al., 1992),

$$x = [\mathrm{Ca}]_{\mathrm{tot}} - [\mathrm{cam}]_{\mathrm{tot}} \frac{K_1 x + 2K_1K_2x^2 + 3K_1K_2K_3x^3 + 4K_1K_2K_3K_4x^4}{1 + K_1x + K_1K_2x^2 + K_1K_2K_3x^3 + K_1K_2K_3K_4x^4}, \quad (10)$$

where x denotes the free $[Ca^{2+}]_i$, $[cam]_{tot}$ the concentration of the buffer (taken to be 0.5 mM; Porter et al., 1993), and $[Ca]_{tot}$ the total Ca^{2+} concentration (free plus bound Ca^{2+}). The macroscopic Ca^{2+} binding constants K_i ($i = 1, 2, 3, 4$) are 200, 800, 70, and 40 mM^{-1} for *Drosophila* calmodulin under approximately physiological conditions (Maune et al., 1992; Table 1). In our simulations, we implemented Eq. 10 describing the steady state, thereby ignoring the kinetic properties of the Ca^{2+} association and dissociation pro-

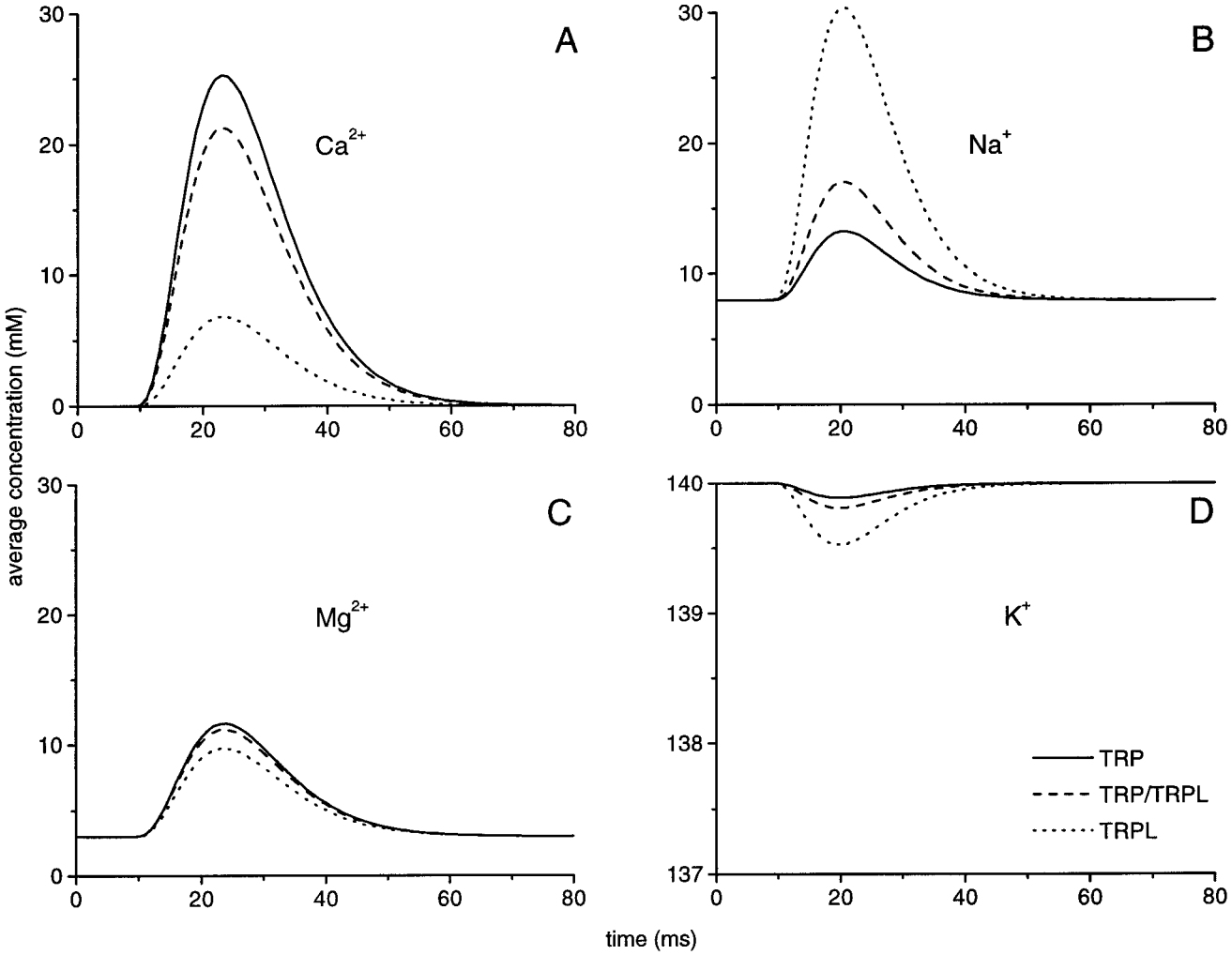

FIGURE 6 Time course of average concentrations of (A) Ca^{2+}, (B) Na^{+}, (C) K^{+}, and (D) Mg^{2+} (assuming that the bump occurs in one microvillus) for three different permeability ratios (Table 2), i.e., the permeability ratio of TRP channels (*solid line*), of a mixture of TRP and TRPL channels (*dashed line*), and of TRPL channels (*dotted line*). Under the physiological conditions used for the calculations, the changes of $[Ca^{2+}]_i$ and $[Na^{+}]_i$, although dependent on the permeability ratio chosen, are in all cases in the millimolar range, as holds for the change of $[Mg^{2+}]_i$. $[K^{+}]_i$ changes only little during a bump, no matter what permeability ratios are chosen.

cesses. This simplification can probably be made without compromise for the association reactions because the time constants of these reactions are in the order of milliseconds or smaller for all four binding sites (Maune et al., 1992; Martin et al., 1992). Also, the dissociation of Ca^{2+} from the low affinity binding sites of calmodulin is fast (800 s^{-1}; Martin et al., 1992). However, the dissociation of Ca^{2+} from the high affinity binding sites might have been overestimated because the rate constant for this reaction is only 17 s^{-1} (Martin et al., 1992).

Calmodulin might be free to diffuse in the microvilli; however, in smooth muscle cells, diffusional freedom of calmodulin is limited (Luby-Phelps et al., 1995). In the microvilli, there are many proteins that bind calmodulin. Some, e.g., TRPL (Warr and Kelly, 1996) and neither inactivation nor other potential C (NINAC) (Porter et al., 1995), possibly bind calmodulin even at low $[Ca^{2+}]_i$, indicating that the effective diffusion constant for calmodulin might indeed be small. We have investigated two extreme cases, one in which the diffusion coefficient of calmodulin is assumed to have the high value $D_{cam} = 100\ \mu m^2 s^{-1}$, which is similar to the diffusion coefficient of the small fluorescent Ca^{2+} indicator fluo-3 (Hall et al., 1997). This diffusion coefficient is assumed to be independent of the amount of Ca^{2+} bound to calmodulin. In the second case, we assumed calmodulin to be immobile. For investigating the effects of Ca^{2+} buffering, we chose the permeability ratios of the TRP channels, because they probably are closest to the permeability ratios found in wild-type photoreceptor cells under physiological conditions (see above).

In Fig. 7, we compare the time courses of the spatially averaged free Ca^{2+} concentrations when considering different assumptions about Ca^{2+} buffering: no Ca^{2+} buffer, an immobile Ca^{2+} buffer, and a mobile Ca^{2+} buffer. Both the

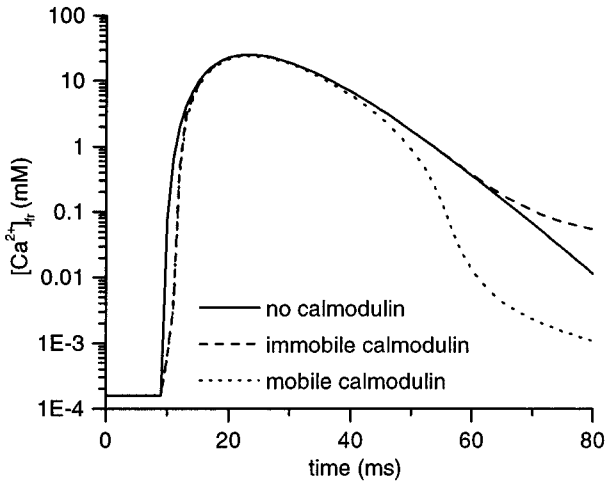

FIGURE 7 Time courses of the spatial average of $[Ca^{2+}]_i$ in a microvillus calculated with different calcium buffer models: no calmodulin present in the microvillus (*solid line*), 0.5 mM immobile calmodulin with 4 Ca^{2+} binding sites (*dashed line*), and 0.5 mM mobile calmodulin with 4 Ca^{2+} binding sites and diffusion coefficient $D_{cam} = 100\ \mu m^2 s^{-1}$ (*dotted line*). The macroscopic binding constants of the 4 binding sites of *Drosophila* calmodulin are taken from Maune et al. (1992). The association and dissociation reactions of Ca^{2+} with the calmodulin are assumed to be in equilibrium and are described by the Adair–Klotz-equation (Eq. 10; see text). The calculations assume the permeability ratios of TRP channels (case 1, Table 2) and that a bump is produced in a single microvillus. The calmodulin influences the dynamics of $[Ca^{2+}]_i$, but has virtually no effect on the peak of $[Ca^{2+}]_i$ reached during a bump.

mobile and the immobile buffer delay the rise of the free Ca^{2+} concentration by ~2 ms compared to a buffer-free situation. However, the peak concentrations reached are virtually independent of the buffering (Fig. 7); the differences found are smaller than 1.0 mM. This shows that the $4 \times 0.5 = 2.0$ mM Ca^{2+}-binding sites offered by calmodulin are saturated with Ca^{2+} at the peak of the Ca^{2+} concentration. As commonly found (e.g., Sala and Hernández-Cruz, 1990; Roberts, 1994), the mobile and the immobile buffer have opposing effects during the decrease of the free Ca^{2+} concentration. An immobile buffer slows the decrease in free Ca^{2+} concentration as the buffer releases the bound Ca^{2+} during the decrease. The mobile buffer, in contrast, increases the speed of the concentration decrease, because it diffuses out of the microvilli together with bound Ca^{2+}, thereby increasing the effective diffusion for Ca^{2+}. In conclusion, the incorporation of a high (2.0-mM Ca^{2+} binding sites) concentration of endogenous buffer does not substantially reduce the rise of free Ca^{2+} concentrations into the millimolar range in the microvilli.

Low affinity, high capacity Ca^{2+} buffer

The phospholipids of membranes bind calcium ions with low affinity (McLaughlin et al., 1981). The surface-to-volume ratio of a microvillus is very large. Therefore, the effective concentration of phospholipids is very high, which could lead to a considerable amount of calcium being buffered by these molecules. In rod photoreceptors, it has been estimated that this effect has dramatic consequences for the diffusion of Ca^{2+} ions in the space between the discs (McLaughlin and Brown, 1981). The effectiveness of membranes as Ca^{2+} buffers depends critically on the phospholipid composition of the membranes, because anionic phospholipids have a higher affinity for Ca^{2+} and, additionally, cause the surface potential to be negative. A negative surface potential leads to an increased concentration of cations at the surface of the membranes, which facilitates their binding to the membranes. However, unlike the discs of vertebrate rods, the microvilli of invertebrate photoreceptor cells seem to have only a small concentration of the principal anionic phospholipid phosphatidylserine (PS) (Paulsen et al., 1983; Zinkler et al., 1985). The rhabdomeric membrane of fly photoreceptor cells contains approximately 50% phosphatidylethanolamine (PE), 25% phosphatidylcholine (PC), and 5% PS. Assuming that each phospholipid occupies an area of $0.7 \cdot 10^{-18}$ m^2 (McLaughlin and Brown, 1981) and that the microvillus membrane only consists of phospholipids, we derive that the effective concentrations for PE, PC, and PS are $[PE]_{tot} = 80$ mM, $[PC]_{tot} = 40$ mM, and $[PS]_{tot} = 8$ mM.

The Gouy–Chapman theory of the diffuse double layer (Israelachvili, 1991) predicts that the surface potential due to the PS lipids at the ionic resting conditions is $\psi_s = -5.5$ mV (Appendix 2). It follows from the Boltzmann equation that such a surface potential increases the concentration of divalent cations at the membrane surface 1.54-fold as compared to the bulk concentrations. To check the significance of the membrane as a calcium buffer, we included low affinity immobile calcium buffers with the Ca^{2+} dissociation constants of the phospholipids ($K_{PE} = K_{PC} = 333.3$ mM and $K_{PS} = 83.3$ mM; McLaughlin et al., 1981) in our model, taking into account the increased Ca^{2+} concentration at the membrane. In the simulations, we assumed that the Ca^{2+} binding reaction to the phospholipids is always in the steady state. The calculations show that inclusion of the phospholipid calcium buffers only slightly reduces the peak calcium concentration from 24 mM to 21 mM, when 0.5 mM mobile calmodulin is assumed to be present. With immobile or no calmodulin present, the effect of the phospholipid buffers is even less significant.

These calculations, however, are an overestimation of the effect of phospholipid Ca^{2+} buffering.

1. The effective phospholipid concentrations used are probably too high because the rhabdomeric membranes contain high amounts of membrane proteins.
2. The surface potential was assumed to stay constant during the simulations. The huge changes in cationic concentrations and the binding of Ca^{2+} to the phospholipids itself, however, would reduce the surface potential and hence the concentration of Ca^{2+} at the membrane surface.
3. Mg^{2+} has similar binding constants to the phospholipids as Ca^{2+} (McLaughlin et al., 1981). Mg^{2+} therefore com-

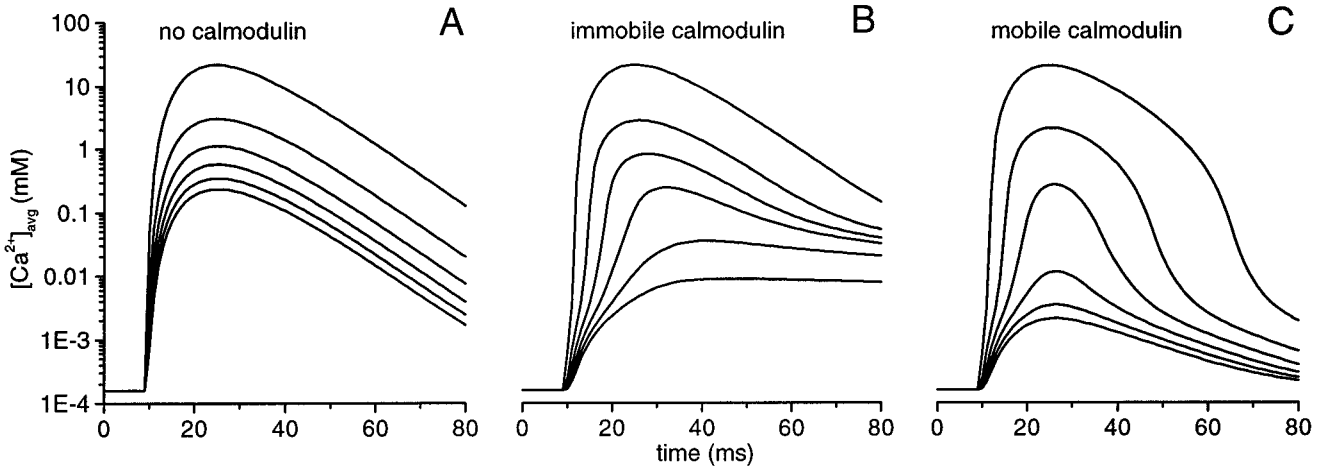

FIGURE 8 Time courses of the (spatial) average of $[Ca^{2+}]_i$ in a microvillus assuming that more than one microvillus participate in a bump. The lines from top to bottom of each panel correspond to 1, 7, 19, 37, 61, and 91 microvilli participating in a bump, respectively. In the calculations, the permeability ratios of TRP channels are assumed (case 1, Table 2). (*A*) No calmodulin; (*B*) 0.5 mM immobile calmodulin with 4 Ca^{2+} binding sites; (*C*) 0.5 mM mobile calmodulin with 4 Ca^{2+} binding sites and a diffusion coefficient $D_{cam} = 100\ \mu m^2 s^{-1}$ is assumed. In all cases, the Ca^{2+} binding to phospholipids is included in the model (see text for details on Ca^{2+} buffers).

petes with Ca^{2+} in binding to phospholipids, an effect that we neglected.

We conclude that the Ca^{2+} buffering by phospholipids does not significantly change the high Ca^{2+} concentrations in the microvilli during a bump.

Number of participating microvilli

Up to now, we have assumed that all the TRP and TRPL channels that are opened during a bump are located in one microvillus. However, it is conceivable that channels in adjacent microvilli, surrounding the microvillus in which the absorption of the photon took place, are also activated. This situation has been demonstrated to occur in the ventral photoreceptor cells of *Limulus* (Stieve, 1986).

In the following, we assume that, in *Drosophila* photoreceptor cells, a fast process transports the signal to channels located in microvilli that are in the vicinity of the microvillus that contains the activated rhodopsin. Assuming the microvilli are hexagonally packed, we obtain $n = 1$, 7, 19, 37, 61, and 91 equally participating microvilli when we stepwise increase the number of participating microvilli, always adding one ring of microvilli. The current per microvillus then becomes $I_m(t) = I(t)/n$ (see Materials and Methods). Using the reduced current per microvillus, I_m, we have calculated the spatially averaged free calcium concentration. We have included the Ca^{2+} buffering by phospholipids and considered the following three cases: no calmodulin (Fig. 8 *A*), immobile calmodulin (Fig. 8 *B*), and mobile calmodulin (Fig. 8 *C*); the quantitative details of the three cases are described above. For quantitative comparison, we plotted the peak values of the free calcium concentrations of each curve of Fig. 8, *A–C* versus the number of microvilli in Fig. 9.

The calculated Ca^{2+} concentrations (Figs. 8 and 9) strongly depend on the number of microvilli participating in the bump. When we do not take buffering by calmodulin into account, the peak of the Ca^{2+} concentrations is inversely proportional to the number of microvilli (Fig. 9); for example, at $n = 91$, the peak of the Ca^{2+} concentration is, consequently, lowered to 0.24 mM. The situation is more

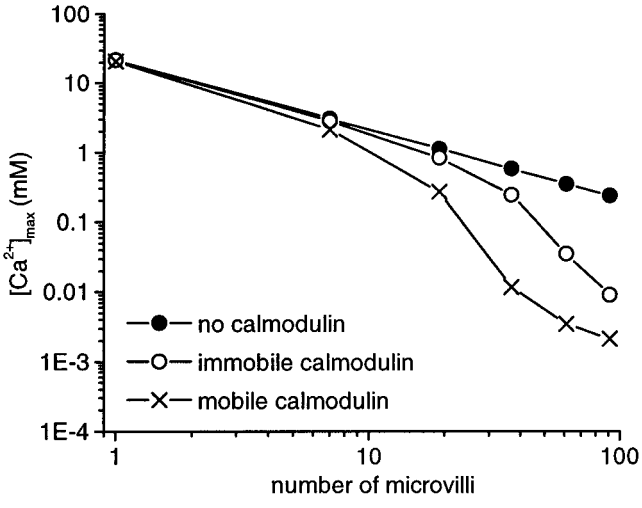

FIGURE 9 Peak values of the spatial average of $[Ca^{2+}]_i$ in the microvillus (from Fig. 8) versus the number of microvilli participating in the bump. Without calmodulin (*solid circles*), the peak of $[Ca^{2+}]_i$ reduces linearly with the number of participating microvilli. The immobile calmodulin (*open circles*) causes an additional reduction of the peak of $[Ca^{2+}]_i$, compared to the situation without calmodulin, when more than 19 microvilli participate. The mobile calmodulin (*crosses*) already causes this additional reduction when more than 7 microvilli are considered. However, when no more than 25 microvilli are assumed to participate in the production of a bump, the peak of the spatially averaged $[Ca^{2+}]_i$ is higher than 80 μM for all buffer models.

complex for the models that include calmodulin: as already shown (Fig. 7), the Ca^{2+} buffering has little effect when assuming that only one microvillus participates. The same occurs when allowing $n = 7$ microvilli to take part at the bump. Further increasing the number of participating microvilli leads to strong nonlinear lowering of free Ca^{2+} concentrations (Figs. 8 and 9), the mobile buffer being more effective in reducing the Ca^{2+} concentrations than the immobile buffer. At $n = 91$ microvilli participating in the bump, the peak Ca^{2+} concentrations (Fig. 9) are 9 and 2 μM for immobile and mobile buffers, respectively. In the Discussion, however, we will argue that it is unlikely that more than 25 microvilli participate in a single bump, leaving more than 80 μM for the peak of the free Ca^{2+} concentration, even when assuming a highly mobile Ca^{2+} buffer with 2.0 mM Ca^{2+} binding sites.

DISCUSSION

In this paper, we calculate the free concentrations of Ca^{2+} (and other ions) inside the microvilli of *Drosophila* photoreceptor cells during a quantum bump. Assuming that all activated channels are situated in a single microvillus, we invariably arrive at free Ca^{2+} concentrations in the millimolar range, regardless of the assumptions made about permeability ratios and Ca^{2+} buffering. In contrast, the calculated free Ca^{2+} concentrations depend strongly on the number of microvilli assumed to share the current of a bump, potentially reducing the free calcium concentration into the micromolar range, when the number of microvilli increases to above 20.

How many microvilli participate in a bump?

Fly photoreceptor cells exposed to bright continuous light stimulation respond with a sustained response that consists of a superposition of bumps, giving rise to shot noise (Wu and Pak, 1978). An analysis of this shot noise in the sheep blowfly *Lucilia* led Howard et al. (1987) to conclude that the maximum number of simultaneously active bumps is as high as the number of microvilli, suggesting that a bump is produced in a single microvillus. However, this analysis was performed on light-adapted photoreceptor cells, and it is not clear that also in dark-adapted cells a single microvillus can sustain a bump. Because bumps in dark-adapted cells are larger than in light-adapted ones (Wu and Pak, 1978), several microvilli might participate in a bump.

The only rhabdomeric photoreceptor cell, for which there is a direct estimate of the number of microvilli participating in a bump, is the ventral photoreceptor cell of the horseshoe crab *Limulus polyphemus*. In this preparation, it has been demonstrated that more than 1000 microvilli participate in a bump (Stieve, 1986). However, phototransduction in *Limulus* ventral photoreceptor cells is, at least quantitatively, different from the phototransduction in *Drosophila* because the bumps of *Limulus* are about 200 times larger, the latency is much longer, and the kinetics of the bump current is much slower (Dorlöchter and Stieve, 1997). In *Limulus*, the light-induced current seems to be at least partly activated by an increase of $[Ca^{2+}]_i$ due to light-induced release of Ca^{2+} from stores (Payne et al., 1986; Ukhanov and Payne, 1995, 1997). This mechanism of activation could not be shown for TRP or TRPL channels in *Drosophila* (Hardie, 1995, 1996). An alternative hypothesis of phototransduction, the capacitative Ca^{2+} entry hypothesis (Hardie and Minke, 1995), has also not received any experimental evidence (Hardie, 1995, 1996; Acharya et al., 1997). It has also been proposed that the activation of TRP and TRPL in *Drosophila* results from conformational changes spreading through a network of transduction proteins connected by the inactivation no other potential D (INAD) protein (Montell, 1998). Recently, polyunsaturated fatty acids have been shown to activate heterologously expressed TRPL channels and have been implicated in the activation of TRP and TRPL channels in vivo (Chyb et al., 1999). Because adjacent microvilli are in close contact with each other (Suzuki et al., 1993), it is conceivable that these fatty acids, produced in the vicinity of the activated rhodopsin, diffuse laterally and across the membrane to neighboring microvilli. Although the rise in $[Ca^{2+}]_i$, the capacitative Ca^{2+} entry, and fatty acid hypothesis straightforwardly allow for many microvilli to participate in a single bump, the conformational change hypothesis rather suggests that all the current of a bump is generated in a single microvillus.

Assuming that mainly TRP channels determine the bump size, the number of channels simultaneously open at the peak of the quantum bump current can be inferred from the single-channel conductance of TRP channels (4 pS; Reuss et al., 1997), the reversal potential (11 mV; Reuss et al., 1997), and the bump size (9 pA; Hardie and Minke, 1995) to be ~27. It has recently been shown that, in *Drosophila* photoreceptor cells, TRP and TRPL do not form heteromultimers with properties different from pure TRP and TRPL channels (Reuss et al., 1997), but it is unknown how many subunits of TRP (or TRPL) form a functional channel. Because there are, on average, ~100 TRP proteins present in a microvillus (Huber et al., 1996a), there would be enough TRP present in a single microvillus to produce the peak current of a bump, even when four TRP proteins were needed to produce a functional channel (Phillips et al., 1992). Therefore, from considering the number of open channels, it seems possible, although by no means necessary, that all channels activated during a bump are localized in a single microvillus. In contrast, it seems unlikely that the open probability of activated TRP channels is so low that the bump is distributed over a large (i.e., >25) number of microvilli.

In conclusion, based on the available evidence, we cannot decide how many microvilli participate in the production of a bump. The more recent hypotheses for the activation of TRP and TRPL favor a small number of microvilli, or even a single microvillus, whereas the number of channels simultaneously open at the peak of the bump indicate that the

number of participating microvilli is unlikely to be higher than 25. We therefore have to conclude that the peak of the free Ca^{2+} concentration reached in the microvilli during a bump is in the range of 0.08–22 mM (Fig. 9).

The effects of reduced calmodulin content

Bumps measured by Scott et al. (1997) and Scott and Zuker (1998a) are much larger than the bumps measured by Hardie and Minke (1995) and Hofstee et al. (1996). This difference in size can be explained by the lack of Mg^{2+} in the bath solution in the measurements of Scott et al. (1997) and Scott and Zuker (1998a), because Mg^{2+} at physiological concentrations is known to impose a 3–5-fold block on TRP channels (Hardie and Mojet, 1995). Furthermore, the calmodulin content of photoreceptor cells in the *Drosophila cam* mutant used by Scott et al. (1997) and Scott and Zuker (1998a) is reduced to 10% of that found in wild-type flies (Scott et al., 1997).

Using the bump measurements of Scott and Zuker (1998a) in the *cam* mutant, we have calculated the Ca^{2+} concentration inside the microvilli (Fig. 10). The larger bumps and the reduced endogenous Ca^{2+} buffer lead to even higher Ca^{2+} concentrations inside the microvilli than those calculated previously. When we assume that the bump is produced in one microvillus, the spatially averaged free Ca^{2+} concentration reaches 75 mM (Fig. 10). Even when assuming 91 microvilli to participate in a bump, Ca^{2+} inside these microvilli peaks at 0.7 mM under these conditions. Taking again 25 microvilli as a reasonable upper bound for the number of participating microvilli, we arrive at 3.0 mM for the peak of $[Ca^{2+}]_i$, showing that, under these unphysiological conditions, the peak of the free Ca^{2+} concentration is in the millimolar range. Since the bumps were approximately normal in shape under these conditions, it seems that the phototransduction machinery can function when exposed to millimolar calcium concentrations.

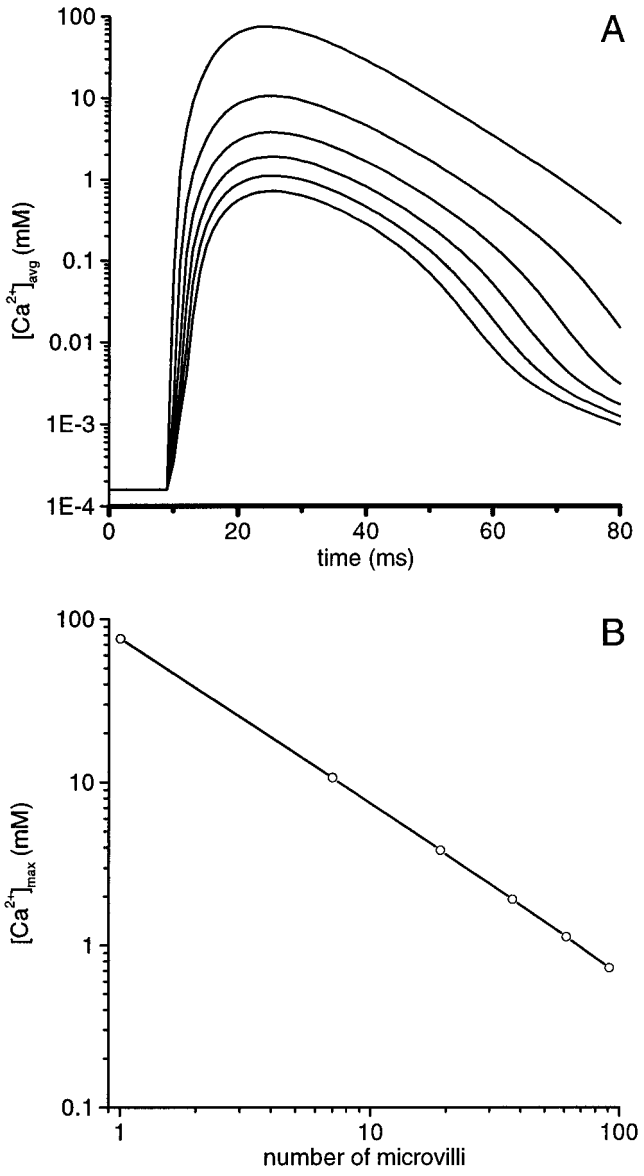

FIGURE 10 (*A*) Time courses of the spatially averaged $[Ca^{2+}]_i$ and (*B*) the peak of the spatially averaged $[Ca^{2+}]_i$ for different number of microvilli calculated for a quantum bump measured in a *cam*-mutant (Scott and Zuker, 1998a). For the calculations, we use the parameters $A = -25$ pA, $\tau = 4$ ms, and $p = 2.38$ in the gamma function. For the Ca^{2+} buffer, we assume 0.05 mM mobile calmodulin with a diffusion constant of $D_{cam} = 100\ \mu m^2 s^{-1}$. The Ca^{2+} binding to phospholipids was included as well (see text for further details). For the intra- and extracellular ion concentrations (mM) we assumed $[Ca^{2+}]_i = 1.6 \cdot 10^{-4}$, $[Ca^{2+}]_o = 1.5$, $[Na^{2+}]_i = 0.1$, $[Na^{+}]_o = 124.0$, $[K^{+}]_i = 135.0$, $[K^{+}]_o = 4.0$, $[Mg^{+}]_i = 2.0$, and $[Mg^{2+}]_o = 0.0$ (Scott and Zuker, 1998a). Under these unphysiological conditions, bumps are much larger due to the lack of extracellular Mg^{2+}. The larger bump amplitude together with the reduced buffer concentration yields much higher values of $[Ca^{2+}]_i$.

The role of Ca^{2+} in shaping the quantum bumps

Ca^{2+} influx has a profound role in shaping the light response of *Drosophila* photoreceptor cells (Hardie, 1991; Ranganathan et al., 1991; Hardie and Minke, 1994). It has been shown that the Ca^{2+} influx causes an early positive feedback and a subsequent negative feedback on TRP channels, and a negative feedback on TRPL channels (Reuss et al., 1997). The positive feedback on TRP channels is extremely rapid (Hardie and Minke, 1994; Hardie, 1995), but its molecular mechanism has not yet been elucidated. The later negative feedback might be dependent on many proteins; a defective response termination has been described in the mutants *inaC* (Ranganathan et al., 1991; Hardie et al., 1993), *inaD* (Shieh and Niemeyer, 1995; Shieh and Zhu, 1996; Shieh et al., 1997; Adamski et al., 1998) and *ninaC* (Porter et al., 1995). Furthermore, the TRP protein has one calmodulin binding site, whereas TRPL has two binding sites (Phillips et al., 1992; Warr and Kelly, 1996), both of which have been shown to be involved in the termination of the light response (Scott et al., 1997). The proteins ePKC (INAC), INAD, NINAC, TRP, and TRPL are all located in the microvilli (Scott and Zuker, 1998b; Montell, 1998) and

therefore are, already during the response to a single photon, exposed to Ca^{2+} concentrations calculated to be in the range between 0.08 and 22 mM. It therefore becomes likely that all available Ca^{2+}-dependent feedback mechanisms are fully activated during the quantum bump, especially because the early positive and the later negative feedback have been shown to be activated by micromolar Ca^{2+} concentrations (Hardie, 1995). The difference, therefore, between the early positive feedback and the later negative feedback should be caused by kinetic differences in the regulatory mechanisms rather than by differences in their Ca^{2+} affinity, already during a single bump. Interestingly, Hardie (1995) provided evidence that the Ca^{2+} affinity of the late negative feedback is actually higher than the Ca^{2+} affinity of the fast positive feedback.

The TRP channels, PLC and ePKC (INAC), are bound together in a supramolecular complex by the INAD protein (Huber et al., 1996a; Tsunoda et al., 1997; Chevesich et al., 1997). This close colocalization has been shown to be important for both activation and inactivation of the phototransduction cascade (Shieh and Niemeyer, 1995; Shieh and Zhu, 1996; Shieh et al., 1997; Tsunoda et al., 1997; van Huizen et al., 1998; Adamski et al., 1998). Because the TRP channels are the major Ca^{2+} channels and the ePKC activity depends strongly on Ca^{2+}, Montell (1998) has suggested that one function of the colocalization in the supramolecular complex is to expose the ePKC rapidly to high Ca^{2+} concentrations. Our results, however, indicate that Ca^{2+} concentrations rise rapidly throughout the microvillus, and therefore, the supramolecular complex may have a different role, possibly the fast and efficient phosphorylation of INAD (Huber et al., 1996b), TRP (Huber et al., 1998) and NINAC (Li et al., 1998) by the ePKC.

The magnitude of the quantum bumps diminishes and the kinetics of the bumps accelerates when the photoreceptor cells are exposed to steady light, i.e., the photoreceptors light adapt (Wu and Pak, 1978; Wong et al., 1982; Howard et al., 1987). These adaptation effects are attributed to an increased $[Ca^{2+}]_i$ (Muijser, 1979; Hardie, 1991, 1995). The levels of $[Ca^{2+}]_i$ reached during prolonged, bright stimulation might be higher than 20 μM (Hardie, 1996; Oberwinkler and Stavenga, 1998), which is still much lower than the microvillar concentrations we calculate during a single bump. Consequently, the Ca^{2+} level reached during light adaptation must drive regulatory processes with a slow time course compared to the duration of a bump. The bump amplitude appears to be pre-set by the Ca^{2+} level due to the light adaptation and to be independent of the Ca^{2+} concentrations transiently reached inside the microvilli during the bump.

Functional constraints of microvillar design

We have argued that the Ca^{2+} concentrations inside the microvilli reach very high values, because the diffusional space inside the microvilli is limited due to their small diameter. Effectively, the microvilli act as extended microdomains (Neher, 1998): the high Ca^{2+} concentrations normally found only close to the channels exist throughout the length of the microvillus. Microvilli, however, necessarily have a small diameter to obtain a high membrane density that allows for high concentrations of rhodopsin molecules, a crucial property for high sensitivity. Furthermore, the flying lifestyle of flies demands phototransduction to be exceptionally rapid, in turn forcing a close colocalization of all components in the signal transduction cascade, including the light-activated channels. The demand for microvilli with small diameters thus potentially conflicts with the necessity to localize the channels to the rhabdomere, because it leads to the extremely high Ca^{2+} concentrations we calculate. The flies seem to make good use of the apparently opposing constraints imposed on the design of the microvilli, as witnessed by the extremely rapid and powerful Ca^{2+}-mediated feedback mechanism acting on the transduction cascade that help to generate a sensitive, fast, and reliable response to a wide variety of light stimuli.

APPENDIX A: DIFFERENCE SCHEME

Because the microvillus length is $L_m = 1.5$ μm and the neck length is $L_n = 0.06$ μm, we divide the microvillus into $N = (L_m + L_n)/L_n = 26$ sections, hence there are $N + 1 = 27$ grid points. The grid points are at $x_k = k\Delta x$, with $k = \{0, \ldots, N\}$.

A second-order numerical scheme for the flux-diffusion equation (Eq. 5) then is

$$\frac{\partial C_0}{\partial t} = -\frac{2}{r_m} j_0 + 2\frac{D}{\Delta x^2}(C_1 - C_0), \tag{A1a}$$

$$\frac{\partial C_k}{\partial t} = -\frac{2}{r_m} j_k + \frac{D}{\Delta x^2}(C_{k-1} - 2C_k + C_{k+1}), \quad 1 < k < N - 1 \tag{A1b}$$

$$\frac{\partial C_{N-1}}{\partial t} = -\frac{2}{r_m}\frac{1}{1+f} j_{N-1} + 2\frac{D}{\Delta x^2}\left(\frac{1}{1+f} C_{N-2} - C_{N-1} + \frac{f}{1+f} C_N\right), \tag{A1c}$$

where C_k is the ion concentration and j_k the flux density at x_k; C_N is the (constant) ion concentration in the cell body and $f = O_n/O_m$ is the ratio of the cross-sections of neck and microvillus. The coefficients containing f involve a modified surface-to-volume ratio at the microvillus-to-neck transition. In this model, we assume that there is no influx of ions at the neck membrane.

The integral in Eq. 9 was calculated with the trapezoidal integration rule.

APPENDIX B: MEMBRANE SURFACE POTENTIAL

The concentration of ions C_s^z at a charged surface is given by the Boltzmann equation,

$$C_s^z = C_0^z e^{-z\beta\psi_s}, \tag{B1}$$

where C_0^z is the bulk concentration of ions with charge z, $\beta = F/(RT)$ and ψ_s is the surface potential. The surface potential can be determined from the Stern equation (Israelachvili, 1991),

$$C_0^{2+}(k^2 - 1) + C_0^{+}(k - 1) + C_0^{-}(k^{-1} - 1) + C_0^{2-}(k^{-2} - 1) - \frac{\sigma(k)^2}{2\varepsilon RT} = 0, \quad \text{(B2)}$$

where, $\varepsilon = 7.08 \cdot 10^{-10}\ \mathrm{C^2N^{-1}m^{-2}}$, $k = e^{-\beta\psi_s}$ and the charge density $\sigma(k)$ is given by

$$\sigma(k) = r_m F C_0^{2+} k^2 \left(\frac{[\mathrm{PE}]_{tot}}{C_0^{2+}k^2 + K_{PE}} + \frac{[\mathrm{PC}]_{tot}}{C_0^{2+}k^2 + K_{PC}} + \frac{[\mathrm{PS}]_{tot}}{C_0^{2+}k^2 + K_{PS}} \right) - \sigma_0, \quad \text{(B3)}$$

where σ_0 is the surface charge density when divalent cations are absent. The surface charge density σ_0 is determined by the 5% negatively charged PS present in the microvillar membrane, because PS is the only major charged phospholipid at physiological pH. Therefore,

$$\sigma_0 = \frac{0.05 \times -1.6 \cdot 10^{-19}}{0.7 \cdot 10^{-18}} = -1.14 \cdot 10^{-2}\ \mathrm{Cm^{-2}}.$$

The values for the ionic concentrations at resting conditions are C_0^{2+} = 3.0 mM (only Mg^{2+}, Table 1), C_0^{+} = 148 mM (Na^+ and K^+, Table 1), C_0^{-} = 140 mM (gluconate, Hofstee et al., 1996) and C_0^{2-} = 3.0 mM (SO_4^{2-}, Hofstee et al., 1996). Mg^{2+} dissociation constants are $K_{PE} = K_{PC}$ = 333 mM and K_{PS} = 125 mM (McLaughlin et al., 1981). Using these values and the effective concentrations of the phospholipids calculated in the text, we obtain a surface potential for the resting conditions of $\psi_s = -5.5$ mV.

REFERENCES

Acharya, J. K., K. Jalink, R. W. Hardy, V. Hartenstein, and C. Zuker. 1997. $InsP_3$ receptor is essential for growth and differentiation but not for vision in *Drosophila. Neuron.* 18:881–887.

Adamski, F. M., M.-Y. Zhu, F. Bahiraei, and B.-H. Shieh. 1998. Interaction of eye protein kinase C and INAD in *Drosophila. J. Biol. Chem.* 273:17713–17719.

Aharon, S., H. Parnas, and I. Parnas. 1994. The magnitude and significance of Ca^{2+} domains for release of neurotransmitter. *Bull. Math. Biol.* 56:1095–1119.

Albritton, N. L., T. Meyer, and L. Stryer. 1992. Range of messenger action of calcium and inositol 1,4,5-trisphosphate. *Science.* 258:1812–1815.

Berridge, M. J. 1998. Neuronal calcium signaling. *Neuron.* 21:13–26.

Boschek, C. B. 1971. On the fine structure of the peripheral retina and lamina ganglionaris of the fly, *Musca domestica. Z. Zellforsch.* 118: 369–409.

Chevesich, J., A. J. Kreuz, and C. Montell. 1997. Requirement for the PDZ domain protein, INAD, for localization of TRP store-operated channel to a signaling complex. *Neuron.* 18:95–105.

Chyb, S., P. Raghu, and R. C. Hardie. 1999. Polyunsaturated fatty acids activate the *Drosophila* light-sensitive channels TRP and TRPL. *Nature.* 397:255–259.

Denk, W., J. R. Holt, G. M. G. Shepherd, and D. P. Corey. 1995. Calcium imaging of single stereocilia in hair cells: localization of transduction channels at both ends of tip links. *Neuron.* 15:1311–1321.

Dorlöchter, M., and H. Stieve. 1997. The *Limulus* ventral photoreceptor light response and the role of calcium in a classic preparation. *Prog. Neurobiol.* 53:451–515.

Gerster, U. 1997. A quantitative estimate of flash-induced Ca^{2+}- and Na^+-influx and Na^+/Ca^{2+}-exchange in blowfly *Calliphora* photoreceptors. *Vision Res.* 37:2477–2485.

Hall, J. D., S. Betarbet, and F. Jaramillo. 1997. Endogenous buffers limit the spread of free calcium in hair cells. *Biophys. J.* 73:1243–1252.

Hardie, R. C. 1985. Functional organization of the fly retina. *In* Progress in Sensory Physiology, Vol. 5, D. Ottoson, editor in chief. Springer, Berlin, Heidelberg, New York, Tokyo. 1–79.

Hardie, R. C. 1991. Whole-cell recordings of the light induced current in dissociated *Drosophila* photoreceptors: evidence for feedback by calcium permeating the light sensitive channels. *Proc. R. Soc. Lond. B.* 245:203–210.

Hardie, R. C. 1995. Photolysis of caged Ca^{2+} facilitates and inactivates but does not directly excite light-sensitive channels in *Drosophila* photoreceptors. *J. Neurosci.* 15:889–902.

Hardie, R. C. 1996. INDO-1 measurements of absolute resting and light-induced Ca^{2+} concentration in *Drosophila* photoreceptors. *J. Neurosci.* 16:2924–2933.

Hardie, R. C., and B. Minke. 1992. The *trp* gene is essential for a light-activated Ca^{2+} channel in *Drosophila* photoreceptors. *Neuron.* 8:643–651.

Hardie, R. C., and B. Minke. 1994. Calcium-dependent inactivation of light-sensitive channels in *Drosophila* photoreceptors. *J. Gen. Physiol.* 105:409–427.

Hardie, R. C., and B. Minke. 1995. Phosphoinositide-mediated phototransduction in *Drosophila* photoreceptors: the role of Ca^{2+} and *trp. Cell Calcium.* 18:256–274.

Hardie, R. C., and M. H. Mojet. 1995. Magnesium-dependent block of the light-activated and *trp*-dependent conductance in *Drosophila* photoreceptors. *J. Neurophys.* 74:2590–2599.

Hardie, R. C., A. Peretz, E. Suss-Toby, A. Rom-Glas, S. A. Bishop, Z. Selinger, and B. Minke. 1993. Protein kinase C is required for light adaptation in *Drosophila* photoreceptors. *Nature.* 363:634–637.

Hofstee, C. A., S. Henderson, R. C. Hardie, and D. G. Stavenga. 1996. Differential effects of *ninaC* proteins (p132 and p174) on light-activated currents and pupil mechanism in *Drosophila* photoreceptors. *Vis. Neurosci.* 13:897–906.

Howard, J., B. Blakeslee, and S. B. Laughlin. 1987. The intracellular pupil mechanism and photoreceptor signal:noise ratios in the fly *Lucilia cuprina. Proc. R. Soc. Lond. B.* 231:415–435.

Huber, A., P. Sander, A. Gobert, M. Bähner, R. Hermann, and R. Paulsen. 1996a. The transient receptor potential protein (Trp), a putative store-operated Ca^{2+} channel essential for phosphoinositide-mediated photoreception, forms a signaling complex with NorpA, InaC and InaD. *EMBO J.* 15:7036–7045.

Huber, A., P. Sander, and R. Paulsen. 1996b. Phosphorylation of the *inaD* gene product, a photoreceptor membrane protein required for the recovery of visual excitation. *J. Biol. Chem.* 271:11710–11717.

Huber, A., P. Sander, A. Gobert, M. Bähner, and R. Paulsen. 1998. The TRP Ca^{2+} channel assembled in a signaling complex by the PDZ domain protein INAD is phosphorylated through the interaction with protein kinase C (ePKC). *FEBS Lett.* 425:317–322.

Israelachvili, J. N. 1991. Intermolecular and Surface Forces. Academic Press, London.

Koch, C., and A. Zador. 1993. The function of dendritic spines: devices subserving biochemical rather than electrical compartmentalization. *J. Neurosci.* 13:413–422.

Kushmerick, M. J., and R. J. Podolsky. 1969. Ionic mobility in muscle cells. *Science.* 166:1297–1298.

Llinás, R., M. Sugimori, and R. B. Silver. 1992. Microdomains of high calcium concentration in a presynaptic terminal. *Science.* 256:677–679.

Llinás, R., M. Sugimori, and R. B. Silver. 1995. The concept of calcium concentration microdomains in synaptic transmission. *Neuropharmacology.* 34:1443–1451.

Li, H.-S., J. A. Porter, and C. Montell. 1998. Requirement for the NINAC kinase/myosin for stable termination of the visual cascade. *J. Neurosci.* 18:9601–9606.

Luby-Phelps, K., M. Hori, J. M. Phelps, and D. Won. 1995. Ca^{2+}-regulated dynamic compartmentalization of calmodulin in living smooth muscle cells. *J. Biol. Chem.* 270:21532–21538.

Lumpkin, E. A., and A. J. Hudspeth. 1995. Detection of Ca^{2+} entry through mechanosensitive channels localizes the site of mechanoelectri-

cal transduction in hair cells. *Proc. Natl. Acad. Sci. USA.* 92: 10297–10301.

Martin, S. R., J. F. Maune, K. Beckingham, and P. M. Bayley. 1992. Stopped-flow studies of calcium dissociation from calcium-binding-site mutants of *Drosophila melanogaster* calmodulin. *Eur. J. Biochem.* 205: 1107–1114.

Maune, J. F., C. B. Klee, and K. Beckingham. 1992. Ca^{2+} binding and conformational change in two series of point mutation to the individual Ca^{2+} binding sites of calmodulin. *J. Biol. Chem.* 8:5286–5295.

McLaughlin, S., and J. Brown. 1981. Diffusion of calcium ions in retinal rods. A theoretical calculation. *J. Gen. Physiol.* 77:475–487.

McLaughlin, S., N. Mulrine, T. Gresalfi, G. Vaio, and A. McLaughlin. 1981. Adsorption of divalent cations to bilayer membranes containing phosphatidylserine. *J. Gen. Physiol.* 77:445–473.

Montell, C. 1998. TRP trapped in fly signalling web. *Curr. Opin. Neurobiol.* 8:389–397.

Muijser, H. 1979. The receptor potential of retinular cells of the blowfly *Calliphora*: the role of sodium, potassium and calcium ions. *J. Comp. Physiol.* 132:87–95.

Neher, E. 1998. Vesicle pools and Ca^{2+} microdomains: new tools for understanding their roles in neurotransmitter release. *Neuron.* 20: 389–399.

Niemeyer, B. A., E. Suzuki, K. Scott, K. Jalink, and C. S. Zuker. 1996. The *Drosophila* light-activated conductance is composed of the two channels TRP and TRPL. *Cell.* 85:651–659.

Oberwinkler, J., and D. G. Stavenga. 1998. Light dependence of calcium and membrane potential measured in blowfly photoreceptors in vivo. *J. Gen. Physiol.* 112:113–124.

Paulsen, R., D. Zinkler, and M. Delmelle. 1983. Architecture and dynamics of microvillar photoreceptor membranes of a cephalopod. *Exp. Eye Res.* 36:47–56.

Payne, R., D. W. Corson, and A. Fein. 1986. Pressure injection of calcium both excites and adapts *Limulus* ventral photoreceptors. *J. Gen. Physiol.* 88:107–126.

Petrozzino, J. J., L. D. Pozzo Miller, and J. A. Connor. 1995. Micromolar Ca^{2+} transients in dendritic spines of hippocampal pyramidal neurons in brain slice. *Neuron.* 14:1223–1231.

Phillips, A. M., A. Bull, and L. Kelly. 1992. Identification of a *Drosophila* gene encoding a calmodulin-binding protein with homology to the *trp* phototransduction gene. *Neuron.* 12:1257–1267.

Porter, J. A., M. Yu, S. K. Doberstein, T. D. Pollard, and C. Montell. 1993. Dependence of calmodulin localization in the retina on the NinaC unconventional myosin. *Science.* 262:1038–1042.

Porter, J. A., B. Minke, and C. Montell. 1995. Calmodulin binding to *Drosophila* NinaC required for termination of phototransduction. *EMBO J.* 14:4450–4459.

Rall, W. 1977. Core conductory theory and cable properties of neurons. *In* Handbook of Physiology. E. R. Kandel, editor. American Physiological Society, Bethesda, MD. 39–97.

Ranganathan, R., G. L. Harris, C. F. Stevens, and C. S. Zuker. 1991. A *Drosophila* mutant defective in extracellular calcium-dependent photoreceptor deactivation and rapid desensitization. *Nature.* 354:230–232.

Ranganathan, R., B. J. Bacskai, R. Y. Tsien, and C. S. Zuker. 1994. Cytosolic calcium transients: spatial localization and role in *Drosophila* photoreceptor cell function. *Neuron.* 13:837–848.

Reuss, H., M. H. Mojet, S. Chyb, and R. C. Hardie. 1997. In vivo analysis of the *Drosophila* light-sensitive channels, TRP and TRPL. *Neuron.* 19:1249–1259.

Roberts, W. M. 1994. Localization of calcium signals by a mobile calcium buffer in frog saccular hair cells. *J. Neurosci.* 14:3246–3262.

Robinson, R. A., and R. H. Stokes. 1959. Electrolyte Solutions, 2nd Ed. Butterworths, London.

Sala, F., and A. Hernández-Cruz. 1990. Calcium diffusion modeling in a spherical neuron. Relevance of buffering properties. *Biophys. J.* 57: 313–324.

Scott, K., Y. Sun, K. Beckingham, and C. S. Zuker. 1997. Calmodulin regulation of *Drosophila* light-activated channels and receptor function mediates termination of the light response in vivo. *Cell.* 91:375–383.

Scott, K., and C. S. Zuker. 1998a. Assembly of the *Drosophila* phototransduction cascade into a signalling complex shapes elementary responses. *Nature.* 395:805–808.

Scott, K., and C. S. Zuker. 1998b. TRP and TRPL and trouble in photoreceptor cells. *Curr. Opin. Neurobiol.* 8:383–388.

Shieh, B.-H., and B. Niemeyer. 1995. A novel protein encoded by the *InaD* gene regulates recovery of visual transduction in *Drosophila. Neuron.* 14:201–210.

Shieh, B.-H., and M.-Y. Zhu. 1996. Regulation of the TRP Ca^{2+} channel by INAD in *Drosophila* photoreceptors. *Neuron.* 16:991–998.

Shieh, B.-H., M.-Y. Zhu, J. K. Lee, I. M. Kelly, and F. Bahiraei. 1997. Association of INAD with NORPA is essential for controlled activation and deactivation of *Drosophila* phototransduction in vivo. *Proc. Natl. Acad. Sci. USA.* 94:12682–12687.

Stieve, H. 1986. Bumps, the elementary excitatory responses of invertebrates. *In* The Molecular Mechanism of Photoreception. H. Stieve, editor. Springer, Berlin, Heidelberg, New York, Tokyo. 199–230.

Suzuki, E., E. Katayama, and K. Hirosawa. 1993. Structure of photoreceptive membranes of *Drosophila* compound eyes as studied by quick-freezing electron microscopy. *J. Electron Microsc.* 42:178–184.

Tsunoda, S., J. Sierralta, Y. Sun, R. Bodner, E. Suzuki, A. Becker, M. Socolich, and C. S. Zuker. 1997. A multivalent PDZ-domain protein assembles signalling complexes in a G-protein-coupled cascade. *Nature.* 388:243–249.

Ukhanov, K., and R. Payne. 1995. Light activated calcium release in *Limulus* ventral photoreceptors as revealed by laser confocal microscopy. *Cell Calcium.* 18:301–313.

Ukhanov, K., and R. Payne. 1997. Rapid coupling of calcium release to depolarization in *Limulus polyphemus* ventral photoreceptors as revealed by microphotolysis and confocal microscopy. *J. Neurosci.* 17: 1701–1709.

van Huizen, R., K. Miller, D. Chen, Y. Li, Z. Lai, R. W. Raab, W. S. Stark, R. D. Shortridge, and M. Li. 1998. Two distantly positioned PDZ domains mediate multivalent INAD–phospholipase C interactions essential for G protein-coupled signaling. *EMBO J.* 17:2285–2297.

Warr, C. G., and L. E. Kelly. 1996. Identification and characterization of two distinct calmodulin-binding sites in the Trpl ion-channel protein of *Drosophila melanogaster. Biochem. J.* 314:497–503.

Wong, F., B. W. Knight, and F. A. Dodge. 1982. Adapting bump model for the ventral photoreceptors of *Limulus. J. Gen. Physiol.* 79:1089–1113.

Wu, C.-F., and W. L. Pak. 1978. Light-induced voltage noise in the photoreceptor of *Drosophila melanogaster. J. Gen. Physiol.* 71: 249–268.

Zinkler, D., J. Bentrop, and R. Paulsen. 1985. Phospholipids of fly photoreceptor membranes: fatty acid and phosphoinositide metabolism. *Verh. Dtsch. Zool. Ges.* 78:303.